Electronic Supplementary Information

Super Flexible, High-efficiency Perovskite Solar Cells Employing Graphene Electrodes: Toward Future Foldable Power Sources

Jungjin Yoon[a,b,†], Hyangki Sung[c,†], Gunhee Lee[a,b], Woohyung Cho[a], Namyoung Ahn[a,b], Hyun Suk Jung[d]* and Mansoo Choi[a,b]*

[a] *Global Frontier Center for Multiscale Energy Systems, Seoul National University, Seoul, 08826, Republic of Korea*

[b] *Department of Mechanical and Aerospace Engineering, Seoul National University, Seoul 08826, Republic of Korea*

[c] *Samsung Display Co. Ltd., Asan 31454, Republic of Korea*

[d] *School of Advanced Materials Science and Engineering, Sungkyunkwan University, Suwon 16419, Republic of Korea*

* E-mail: mchoi@snu.ac.kr (M. Choi), hsjung1@skku.edu (H. S. Jung)

† These authors contributed equally to this work.

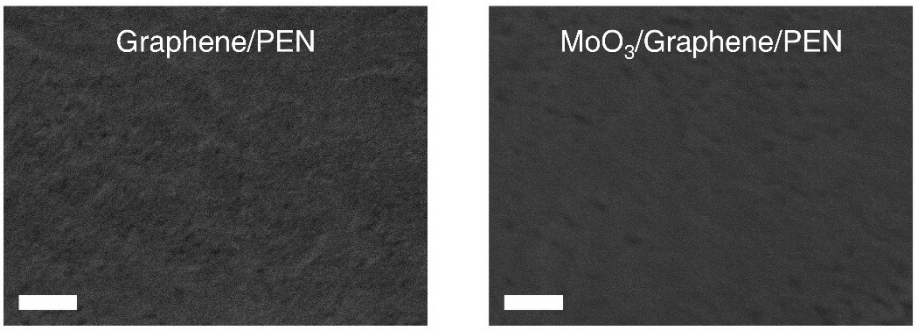

Figure S1. Plane-view SEM images of graphene/PEN surface. Graphene/PEN (left) and MoO_3/Graphene/PEN (right). (Scale bar: 100 nm)

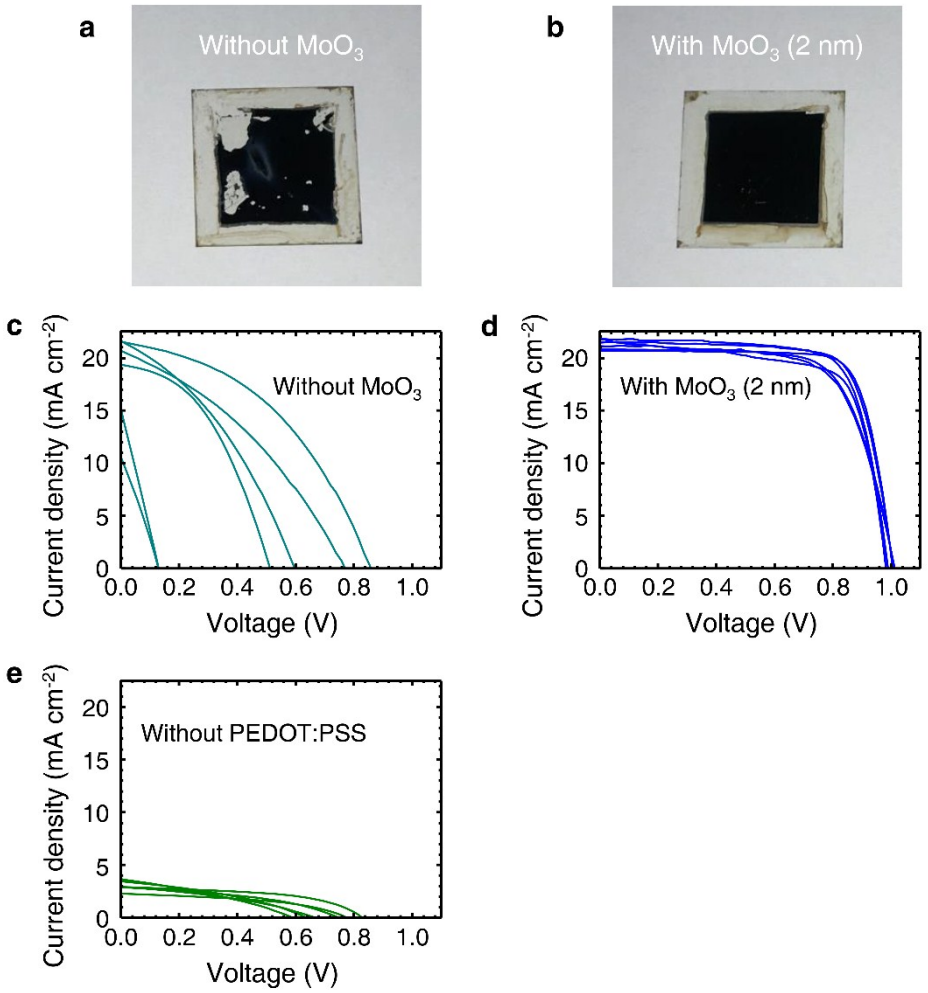

Figure S2. Influence of the presence of MoO_3 on the graphene-based flexible solar cell performance. (a-b) Photograph of perovskite layer coated on (a) PEDOT:PSS/Graphene/PEN, (b) PEDOT:PSS/MoO_3/Graphene/PEN. (c-e) *J-V* curves of devices (c) without MoO_3, (d) with MoO_3, and (e) with only 2 nm-thick MoO_3 (without PEDOT:PSS), respectively.

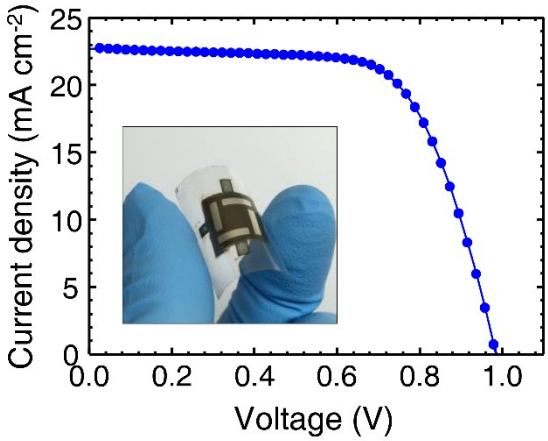

Gr-Mo/PEN device	
Metal electrode area (mm^2)	**9.0**
V_{OC} (V)	0.98
J_{SC} ($mA\ cm^{-2}$)	22.8
FF	0.67
PCE (%)	15.0

Figure S3. Photovolatic performance of the Gr-Mo/PEN device with larger active area. A *J-V* curve (left) and a summarized table (right) of the Gr-Mo/PEN device with a metal electrode area of 9.0 mm^2. During the *J-V* measurement, the device was covered with a shadow mask having aperture area of 7.54 mm^2 to minimize any edge effects. Inset photograph shows the complete device.

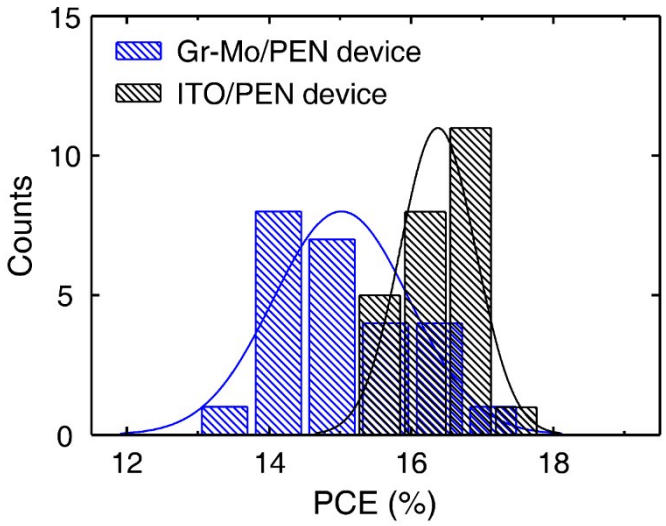

Figure S4. PCE histogram of 25 flexible devices for each electrode type. Good reproducibility of high efficiency with over 15.0% and 16.4% PCEs for the half of Gr-Mo/PEN and ITO/PEN devices, respectively, was exhibited.

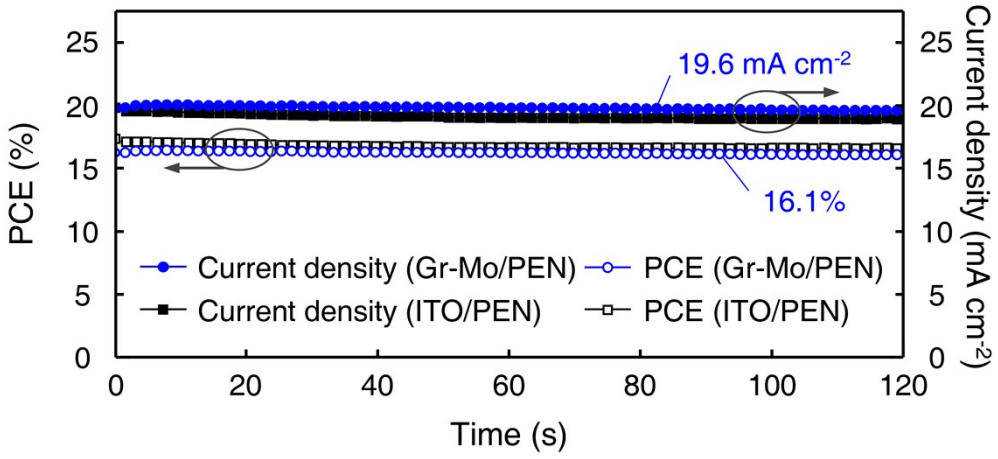

Figure S5. Steady-state current density and stabilized power output of flexible perovskite solar cells with different transparent electrode types. The Gr-Mo/PEN device generated a steady-state current density of 19.6 mA cm^{-2}, which corresponded to a stabilized power output of 16.1 mW cm^{-2}. Whereas, the ITO/PEN device yielded a steady-state current density of 18.9 mA cm^{-2} and a stabilized power output of 16.6 mW cm^{-2}. Each current density was measured under the voltages at the maximum power points; 0.82 V for the graphene-based and 0.88 V for the ITO-based device, respectively.

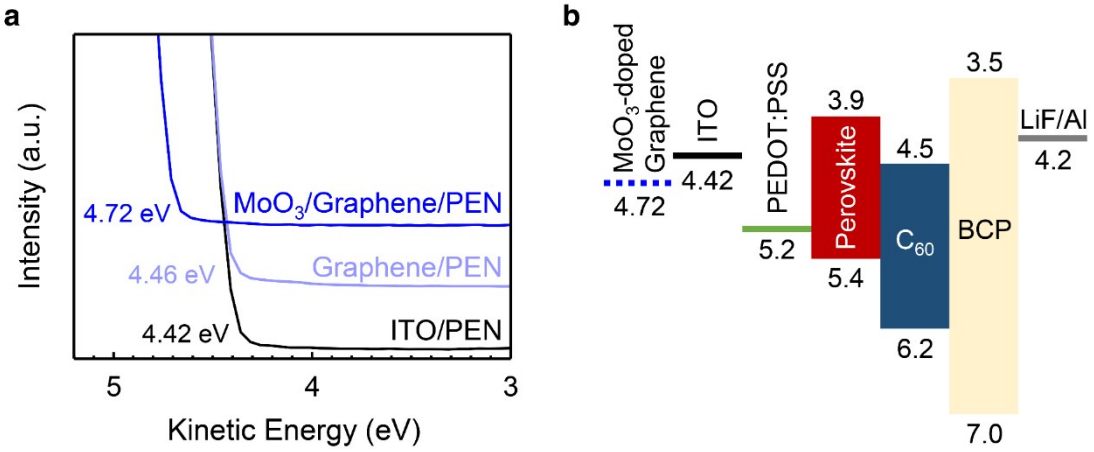

Figure S6. UPS measurement and energy level diagram. (**a**) UPS spectra and derived work functions of the MoO_3 (2 nm)/Graphene/PEN, as-prepared Graphene/PEN, and ITO/PEN substrates, respectively. (**b**) A schematic energy level diagram of the inverted perovskite solar cells fabricated in this work. The energy levels except graphene and ITO were taken from Jeng et al.[1]

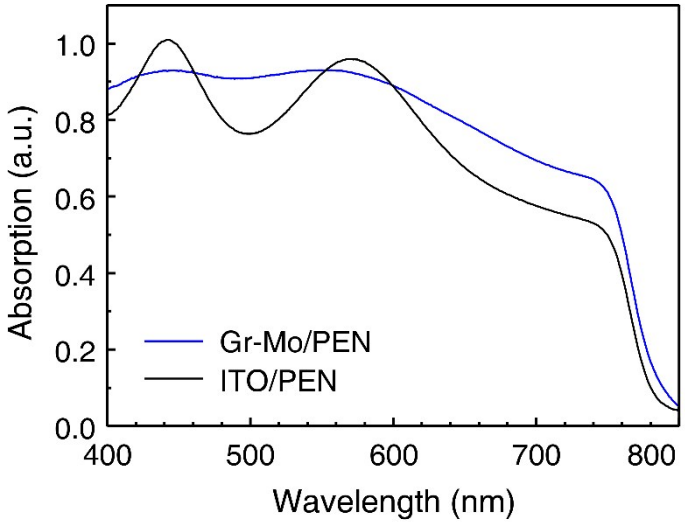

Figure S7. Absorption spectra of perovskite. Perovskite layer coated on PEDOT:PSS/Gr-Mo/PEN (blue) and PEDOT:PSS/ITO/PEN (black).

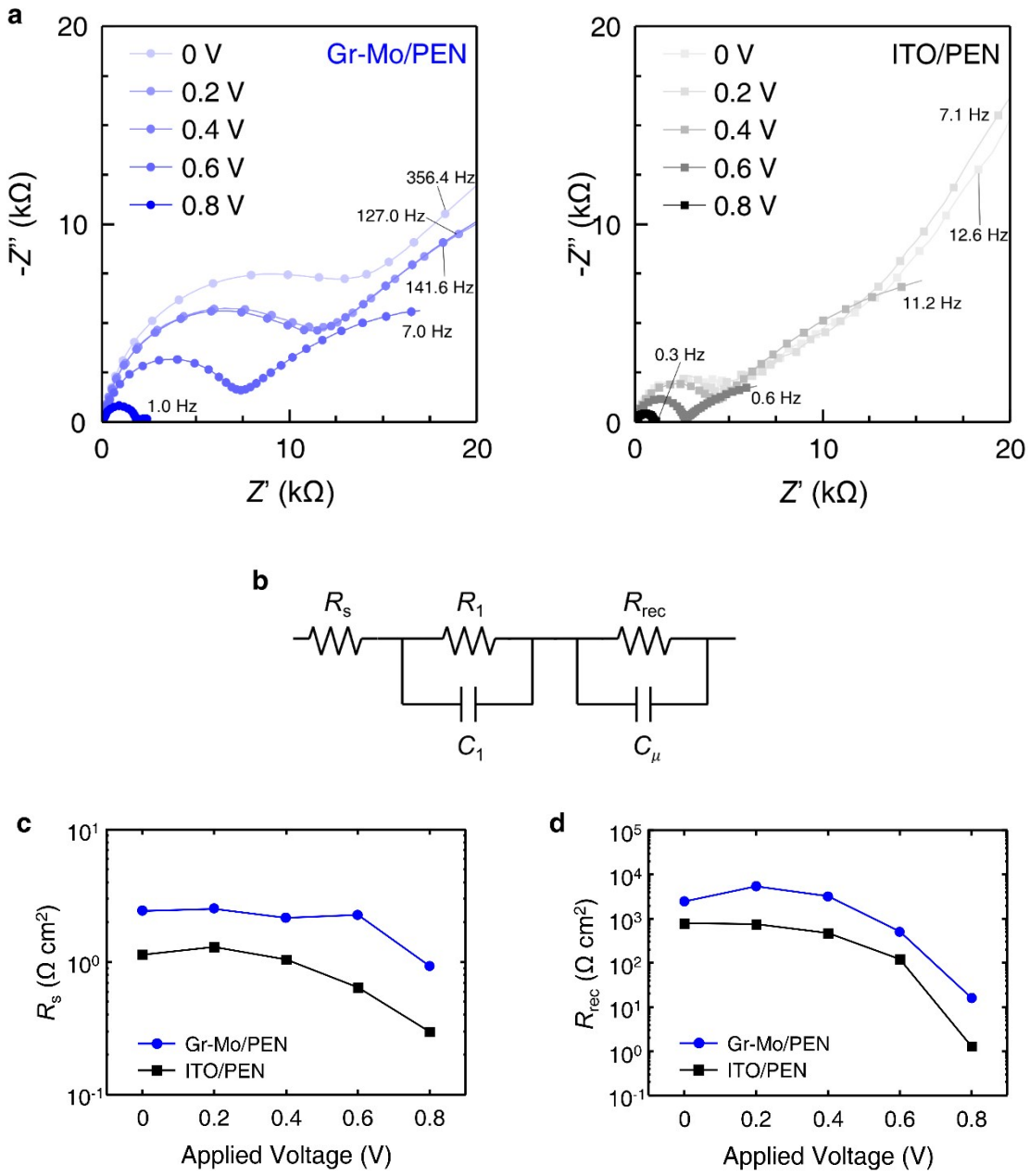

Figure S8. Electrochemical impedance spectroscopy (EIS) analysis for Gr-Mo/PEN or ITO/PEN devices. (**a**) Nyquist plots measured under various voltage conditions (0, 0.2, 0.4, 0.6, and 0.8 V) at one-sun illumination in the frequency range of 1 MHz to 0.05 Hz. (**b**) The equivalent circuit used to fit the results in (**a**). Here, R_s denotes the series resistance and R_{rec} the recombination resistance. The charge collection and recombination events are represented by two resistance-capacitance (*R*-*C*) components[2]; the R_1-C_1 component is for materials or interfaces and the R_{rec}-C_μ component is for the bulk perovskite layer. (**c**)-(**d**) The relation of the

corresponding (**c**) series resistance (R_s) and (**d**) recombination resistance (R_{rec}) with the applied voltage.

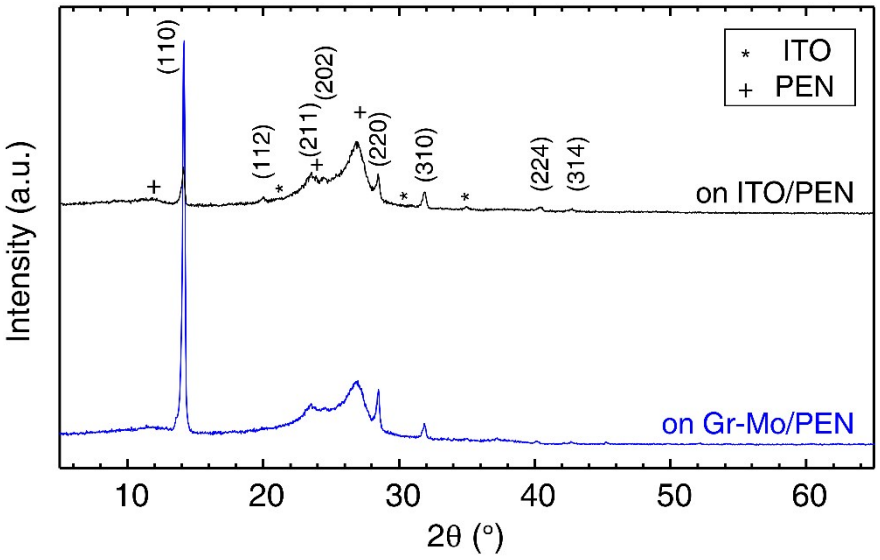

Figure S9. Comparison of the X-ray diffraction patterns. X-ray diffraction (XRD) patterns of the $MAPbI_3$ layers fabricated on the PEDOT:PSS/ITO/PEN and PEDOT:PSS/MoO_3/Graphene/PEN substrates. All the peaks for the $MAPbI_3$ films were presented in the patterns for the both substrates. The peak intensity of the (110) plane was observed to be much stronger from the graphene substrate, compared to the ITO substrate, which was accountable for the preferred grain orientation of the perovskite film.

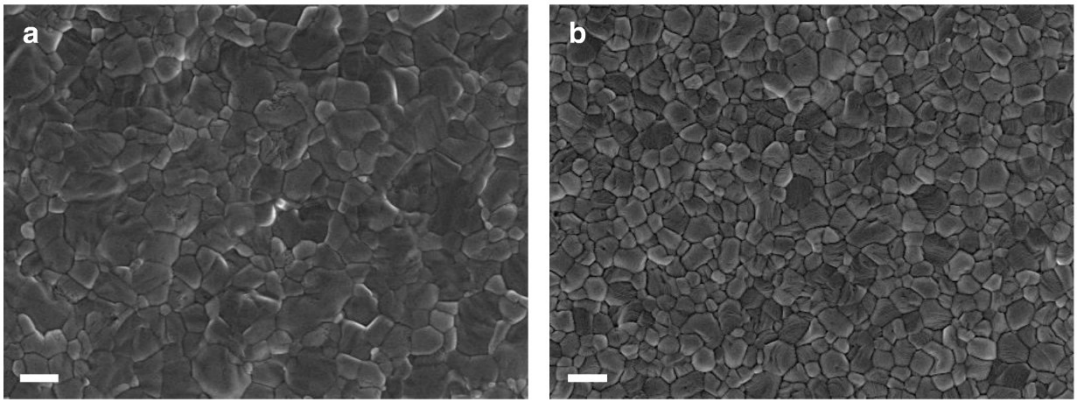

Figure S10. Plane-view SEM images of $MAPbI_3$ layer. (**a-b**) SEM images of the perovskite layers fabricated on (**a**) PEDOT:PSS/MoO_3/Graphene/PEN and (**b**) PEDOT:PSS/ITO/PEN (scale bar, 500 nm).

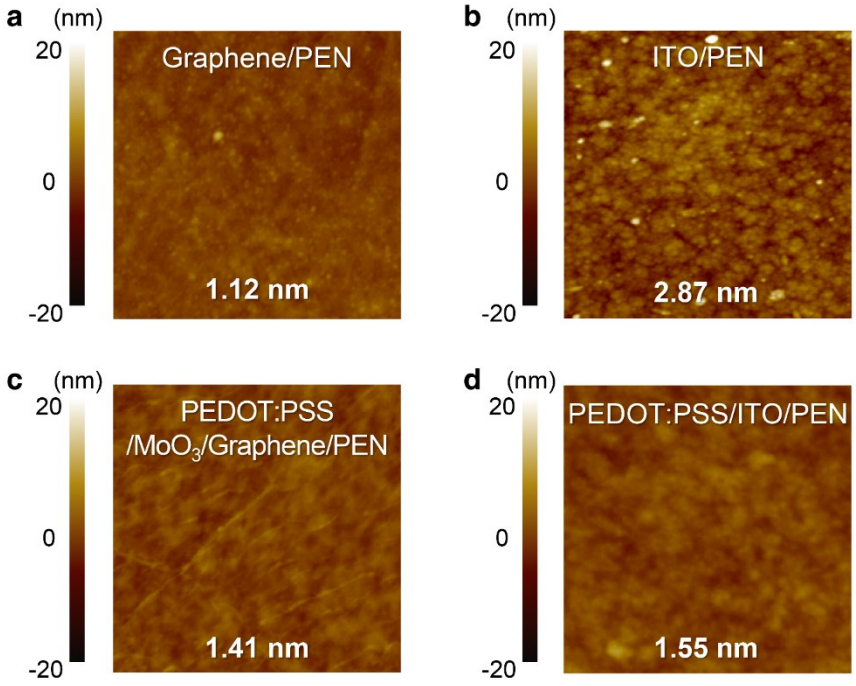

Figure S11. AFM topography images. (**a-d**) The AFM topography images (1.5 μm × 1.5 μm) of (**a**) as-prepared graphene, (**b**) ITO, (**c**) PEDOT:PSS/MoO_3 (2 nm)/Graphene, and (**d**) PEDOT:PSS/ITO/PEN. The calculated surface root-mean-square roughness values were indicated in each image.

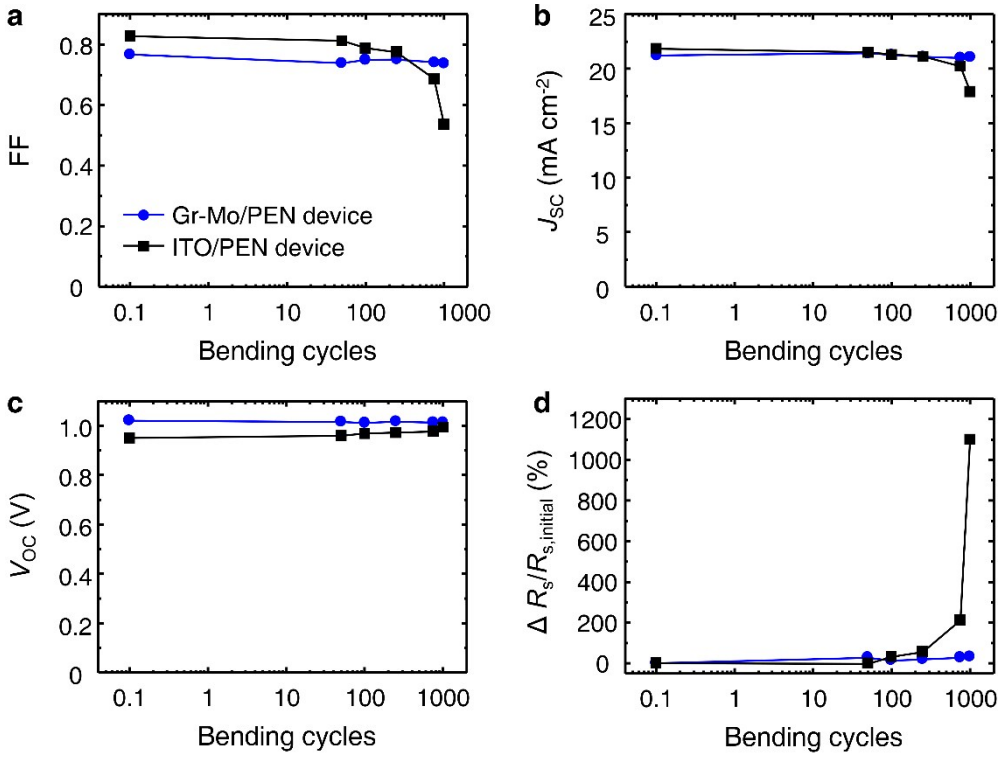

Figure S12. Changes of photovoltaic parameters as function of bending cycles. (**a-d**) The changes of (**a**) FF, (**b**) J_{SC}, (**c**) V_{OC}, and (**d**) $\Delta R_s/R_{s,initial}$ of the flexible devices with each electrode type as a function of bending cycles with a fixed bending radius of 4 mm.

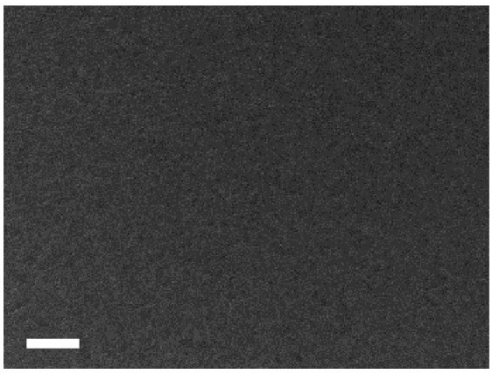

Figure S13. Large-scale SEM image of perovskite film on PEDOT:PSS/Gr-Mo/PEN substrate. The substrate was bent 5000 times with bending radius of 2 mm. There were no observable cracks generated on perovskite surface. (Scale bar: 10 μm)

Reference	Transparent electrode	PCE (%)	Durability test		
		Forward / Reverse scan	Bending radius (mm)	Bending cycles	PCE_{final} /$PCE_{initial}$ (%)
This work	Graphene	16.3 / 16.8	2	5000	85
			4	5000	88
	ITO	17.2 / 17.3	4	1000	30
[3]	Ag mesh/PH1000	13.7 / 14.2	5	5000	95
[4]	PEDOT:PSS	10.78 / 10.89	1	1000	97
[5]	Ni	- / 10.3	50	200	93
[6]	PEDOT:PSS	- / 8.6	2	2000	73
[7]	ITO	15.48 / 16.80	5	200	85
[8]	ITO	- / 14.78	4	200	30
[9]	ITO	15.76 / 16.09	5	300	91
[10]	ITO	10.46 / 11.11	4	1000	50
[11]	ITO	14.2 / 14.4	10	600	60
[12]	ITO	- / 14.53		100	80
[13]	ITO	11.7 / 15.3		300	95

Table S1. Literature comparisons of flexible perovskite solar cells. Literature comparison of the PCEs under different scan directions and the results of the mechanical durability test of flexible perovskite solar cells prepared with different types of transparent electrodes.

	Sheet resistance (Ω sq $^{-1}$)		
	ITO/PEN	**Graphene/PEN**	**MoO_3/Graphene/PEN**
Average	13.3	1260.0	552.0
Standard deviation	1.3	156.3	24.2

Table S2. Sheet resistance of flexible transparent electrodes. The sheet resistances of the as-prepared ITO/PEN, graphene/PEN and MoO_3-doped graphene/PEN substrates measured with a four-point probe were summarized. Deposition of the 2 nm-thick MoO_3 layer lowered the sheet resistance of graphene by ~2.3 times. The average and the standard deviation values were calculated from the sheet resistance values of 4 substrates.

References

1. J. Y. Jeng, Y. F. Chiang, M. H. Lee, S. R. Peng, T. F. Guo, P. Chen and T. C. Wen, *Advanced Materials*, 2013, **25**, 3727-3732.
2. E. J. Juarez-Perez, M. Wuβler, F. Fabregat-Santiago, K. Lakus-Wollny, E. Mankel, T. Mayer, W. Jaegermann and I. Mora-Sero, *The journal of physical chemistry letters*, 2014, **5**, 680-685.
3. Y. Li, L. Meng, Y. M. Yang, G. Xu, Z. Hong, Q. Chen, J. You, G. Li, Y. Yang and Y. Li, *Nature communications*, 2016, **7**.
4. M. Park, H. J. Kim, I. Jeong, J. Lee, H. Lee, H. J. Son, D. E. Kim and M. J. Ko, *Advanced Energy Materials*, 2015, **5**.
5. J. Troughton, D. Bryant, K. Wojciechowski, M. J. Carnie, H. Snaith, D. A. Worsley and T. M. Watson, *Journal of Materials Chemistry A*, 2015, **3**, 9141-9145.
6. K. Sun, P. Li, Y. Xia, J. Chang and J. Ouyang, *ACS applied materials & interfaces*, 2015, **7**, 15314-15320.
7. C. Wang, D. Zhao, C. R. Grice, W. Liao, Y. Yu, A. Cimaroli, N. Shrestha, P. J. Roland, J. Chen and Z. Yu, *Journal of Materials Chemistry A*, 2016.
8. M. Park, J.-Y. Kim, H. J. Son, C.-H. Lee, S. S. Jang and M. J. Ko, *Nano Energy*, 2016, **26**, 208-215.
9. D. Yang, R. Yang, X. Ren, X. Zhu, Z. Yang, C. Li and S. F. Liu, *Advanced Materials*, 2016.
10. B. J. Kim, D. H. Kim, Y.-Y. Lee, H.-W. Shin, G. S. Han, J. S. Hong, K. Mahmood, T. K. Ahn, Y.-C. Joo and K. S. Hong, *Energy & Environmental Science*, 2015, **8**, 916-921.
11. J. W. Jo, M. S. Seo, M. Park, J. Y. Kim, J. S. Park, I. K. Han, H. Ahn, J. W. Jung, B. H. Sohn and M. J. Ko, *Advanced Functional Materials*, 2016.
12. H. Zhang, J. Cheng, F. Lin, H. He, J. Mao, K. S. Wong, A. K.-Y. Jen and W. C. Choy, *ACS nano*, 2015, **10**, 1503-1511.
13. S. S. Shin, W. S. Yang, J. H. Noh, J. H. Suk, N. J. Jeon, J. H. Park, J. S. Kim, W. M. Seong and S. I. Seok, *Nature communications*, 2015, **6**.